

SMART WING SUPERSONIC AND HYPERSONIC AEROELASTICITY

R Moosavi

School of Physics, Engineering & Computer Science, Department of Engineering & Technology,
Centre for Engineering Research, University of Hertfordshire, Hatfield, AL10 9AB, UK

Keywords: Aeroelasticity, Smart Wing, Supersonic Flow

Abstract: In the present paper, aeroelastic phenomena of a smart wing in supersonic and hypersonic flows are investigated to represent the flutter alleviation due to piezoelectric effect. Using nonlinear aerodynamic model, a smart wing with pitch and plunge DOFs is simulated. The equations of motion can be obtained by using the Lagrange's equations and the Kirchhoff's law. To calculate aerodynamic forces acting on the smart wing in supersonic flow, piston theory can be implemented to model airflow by a quasi-steady compressible method. The complete nonlinear aeroelastic smart wing system can be obtained and divergence and flutter speeds are calculated accordingly.

2 INTRODUCTION

Aeroelastic analysis of a modern wing in supersonic and hypersonic regimes is crucial. The ability to control the aeroelastic instability due to flexibility is very important to reach the desired high aerodynamic performance in a wing design [1, 2]. Obviously, one important aeroelastic analysis is flutter resulting from merging of two or more vibration modes during flight. The flutter phenomenon can reduce the flight envelope or even make a redesign of the wing necessary. Appearing flutter can compromise not only the long-term durability of the wing structure, but also the flight performance, operational safety, and energy efficiency of the aircraft. Hence, postponing flutter is crucial for the modern airplane [3-7].

Using smart materials in wing structures has been performed for many years. Although there are different smart materials, piezoelectric materials have received the most attention. Considering the direct and inverse piezoelectric effects of piezoelectric materials, they can perform as sensors and/or actuators on a wing, respectively. In fact, they can be used as actuators and dampers to manage the aeroelastic behaviour of the wing. One effective way to avoid redesign the wing is to use piezoelectric materials to significantly delay the flutter [8]. Adding a shunt circuit to a piezoelectric material can create a piezopatch to modify effectively the wing aeroelastic behaviour. Previously, there were practical limits in the low frequency range like the one typically existing in aeroelastic phenomena due to the large required inductance in passive aeroelastic control. However, nowadays, it is possible to have a small inductor integrated into a piezopatch dedicated to aeroelastic control [9-12]. Since standard inductors usually have too large internal resistance for resonant shunt application, they are not a practical component to integrate into a piezopatch. Implementing closed magnetic circuits with high permeability materials allows the design of large inductance inductors with high quality factors.

The use of shunted piezopatch permits to have damping augmentation in wing structure without causing any instability yet. In addition, they need little to no power and are simple to apply. Their necessary hardware is the piezoelectrics and a simple electric circuit including a capacitor, inductor, and resistor. The shunted piezopatch can control aeroelastic vibration of wing by consuming the energy created from wing vibrations. In fact, it can reduce the vibrations of specific modes and frequencies.

In this paper, the effect of piezoelectric material on increasing the flutter speed in supersonic and hypersonic flow is investigated in detail by considering a simple aeroelastic system. The system is a 2D double wedged wing with piezoelectric patch which has plunge and pitch degrees of freedom (DOF) as well as with high-speed nonlinear aerodynamic forces. The objective of this work is to represent the role of piezoelectric patches that can influence substantially a simple aeropiezoelectric system. Section 2 explains high speed smart wing model by driving the governing equation of motion of the wing. In section 3, high speed nonlinear aerodynamic model is presented to obtain applied aerodynamic load on the wing. Section 4 includes high speed nonlinear aeroelastic model to obtain aeroelastic system equations. Solving procedure is represented in section 5 by implementing amplitude-based iteration scheme on the nonlinear aeroelastic system of equations. Finally, results are given in section 6.

3 HIGH SPEED SMART WING MODEL

A smart wing including plunge and pitch degrees of freedom is shown in Fig. 1. The model contains a double wedge airfoil with two piezoelectric patches one in the plunge DOF and the other one in the pitch DOF. The system has the plunge and pitch degrees of freedom (DOF) indicated by h , α , q_h and q_α , respectively. The equations of motion can be obtained by using the Lagrange's equations and the Kirchoff's law as

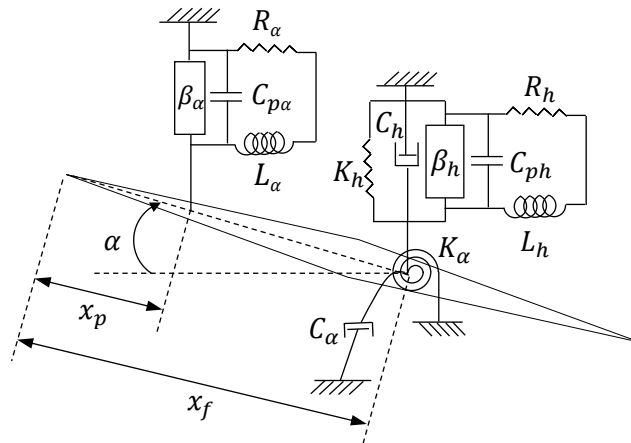


Fig. 1 A high-speed smart wing with pitch and plunge DOF

$$\begin{cases} m\ddot{h} + S_{\alpha h}\ddot{\alpha} + C_h\dot{h} + K_h h - \beta_h q_h = -L \\ S_{\alpha h}\ddot{h} + I_\alpha\ddot{\alpha} + C_\alpha\dot{\alpha} + K_\alpha\alpha - \beta_\alpha q_\alpha = M_{xf} \\ L_h\ddot{q}_h + R_h\dot{q}_h + \frac{1}{C_{ph}}q_h - \beta_h h = 0 \\ L_\alpha\ddot{q}_\alpha + R_\alpha\dot{q}_\alpha + \frac{1}{C_{p\alpha}}q_\alpha - \beta_\alpha(x_f - x_p)\alpha = 0 \end{cases} \quad (1)$$

where

m	mass
\ddot{h}	plunge acceleration
$S_{\alpha h}$	static mass moment of the wing around the pitch axis x_f
$\ddot{\alpha}$	pitching acceleration
C_h	plunge structural damping
\dot{h}	plunge velocity
K_h	plunge structural stiffness
β_h	plunge electromechanical coupling
q_h	plunge electric charge
L	lift
I_α	mass moment of inertia
C_α	pitching structural damping
$\dot{\alpha}$	pitching velocity
K_α	pitching structural stiffness
α	pitching angle
β_α	pitch electromechanical coupling
q_α	pitch electric charge
M_{xf}	pitching moment of the wing around the pitch axis x_f
L_h	plunge inductance of piezoelectric material
\ddot{q}_h	rate of the plunge electrical current
R_h	plunge resistance of piezoelectric material
\dot{q}_h	plunge electrical current
C_{ph}	plunge capacitance of piezoelectric material
h	plunge displacement
L_α	pitch inductance of piezoelectric material

\ddot{q}_α	rate of the pitch electrical current
R_α	pitch resistance of piezoelectric material
\dot{q}_α	pitch electrical current
$C_{p\alpha}$	pitch capacitance of piezoelectric material
x_f	pitch axis
x_p	piezoelectric axis

The plunge electromechanical coupling, β_h , depends on the plunge coupling coefficient, e_h , and the plunge capacitance, C_{ph} , and it can be calculated by $\beta_h = e_h/C_{ph}$. In addition, the pitch electromechanical coupling, β_α , depends on the pitch coupling coefficient, e_α , and the pitch capacitance, $C_{p\alpha}$, and it can be calculated by $\beta_\alpha = e_\alpha/C_{p\alpha}$.

Considering nonlinear piston theory, the lift and moments in Eq. (1) can be obtained in the following section.

3 HIGH SPEED NONLINEAR AERODYNAMIC MODEL

To calculate aerodynamic forces acting on the smart wing from low supersonic to hypersonic speeds up to the limit of Newton flow, piston theory can be implemented to model airflow by a quasi-steady compressible method [13, 14]. Consider a supersonic airflow with density ρ_∞ , pressure p_∞ , and airspeed U_∞ . The airflow has the sound speed $a_\infty = \sqrt{\gamma p_\infty/\rho_\infty}$, compressibility ratio $\gamma = 1.4$, and Mach number $M_\infty = U_\infty/a_\infty$. The upper or lower surface pressure distribution of the wing can be defined by piston theory as follows

$$p_{u,l}(x, t) = p_\infty \left(1 + \frac{\gamma - 1}{2} \frac{w_{u,l}}{a_\infty} \right)^{2\gamma/(\gamma-1)} \quad (2)$$

where $w_{u,l}$ denotes the downwash velocity and subscripts u and l represent the upper and lower surface, respectively. The application of piston theory is for airflow with high Mach numbers, small disturbances, and quasi-steady conditions. It is possible to satisfy these three conditions if at all times [15]

$$M_\infty \frac{w_{u,l}}{U_\infty} < 1 \quad \text{and} \quad kM_\infty \frac{w_{u,l}}{U_\infty} < 1 \quad (3)$$

where $k = \omega c/U_\infty$ is the reduced frequency. Usually, the lower Mach number limit is $M_\infty \geq 1.3$. Using the instantaneous wing shape, the downwash velocity, $v_{u,l}(x, t)$, can be calculated as

$$w_u = - \left(\dot{v}_u + U_\infty \frac{\partial v_u}{\partial x} \right) \quad (4a)$$

$$w_l = \left(\dot{v}_l + U_\infty \frac{\partial v_l}{\partial x} \right) \quad (4b)$$

The wing geometric shape and its displacements in two DOF, plunge h and pitch α , have contributions to the instantaneous wing shape. The wing instantaneous shape can be presented by [16, 17]

$$v_u = h + (x - x_f)\alpha - y_u(x) \quad (5a)$$

$$v_l = h + (x - x_f)\alpha - y_l(x) \quad (5b)$$

where $y_{u,l}(x)$ is the upper and lower surface geometric shape of the wing.

Using $\Delta p(x, t) = p_l(x, t) - p_u(x, t)$, one can calculate the pressure difference across the wing. Then the time dependent lift and moment around the wing pitch axis are obtained by

$$l(t) = \int_0^c \Delta p(x, t) dt \quad (6a)$$

$$m_{x_f}(t) = - \int_0^c \Delta p(x, t)(x - x_f) dt \quad (6b)$$

respectively. Due to existing the irrational exponent $2\gamma/(\gamma - 1)$ in Eq. (2), there is no analytical solution for Δp . To overcome this problem, a binomial expansion can be applied to the bracket term in Eq. (2) which leads to

$$p_{u,l}(x, t) = p_\infty \left(1 + \gamma \frac{w_{u,l}}{a_\infty} + \frac{\gamma(\gamma + 1)}{4} \left(\frac{w_{u,l}}{a_\infty} \right)^2 + \frac{\gamma(\gamma + 1)}{4} \left(\frac{w_{u,l}}{a_\infty} \right)^3 + \dots \right) \quad (7)$$

Implementing a correction factor $\lambda = M_\infty / \sqrt{M_\infty^2 - 1}$ to $w_{u,l}/a_\infty$ in Eq. (2) and (7), piston theory can be applicable throughout the low subsonic to hypersonic flow. Then Eq. (7) becomes

$$p_{u,l}(x, t) = p_\infty \left(1 + \gamma \frac{w_{u,l}\lambda}{a_\infty} + \frac{\gamma(\gamma + 1)}{4} \left(\frac{w_{u,l}\lambda}{a_\infty} \right)^2 + \frac{\gamma(\gamma + 1)}{4} \left(\frac{w_{u,l}\lambda}{a_\infty} \right)^3 \right) \quad (8)$$

where only terms up to third order are considered in the modified equation. If the airfoil is symmetric or its thickness is negligible, $w_u = -w_l$ in Eq. (4) and (5). Then the pressure difference is reduced to

$$\Delta p(x, t) = \frac{4\lambda q_\infty}{M_\infty} \left(\frac{w_l}{U_\infty} + \frac{\gamma + 1}{12} \lambda^2 M_\infty^2 \left(\frac{w_l}{U_\infty} \right)^3 \right) \quad (9)$$

where $q_\infty = 1/2 \rho_\infty U_\infty^2$ is the dynamic pressure of free stream. If the airfoil thickness is negligible, w_l/U_∞ can be written as

$$\frac{w_l}{U_\infty} = \frac{\dot{h}}{U_\infty} + (x - x_f) \frac{\dot{\alpha}}{U_\infty} + \alpha \quad (10)$$

Substituting Eq. (9) into Eqs. (6), the lift and moment include 10 nonlinear terms and are calculated

$$\begin{aligned} l(t) = & \frac{4\lambda q_\infty}{M_\infty} \left(\frac{\dot{h}}{U_\infty} + S' \frac{\dot{\alpha}}{U_\infty} + \alpha \right) + \frac{(\gamma + 1)\lambda^3 M_\infty q_\infty c}{3} \left(\left(\frac{\dot{h}}{U_\infty} \right)^3 + J'_\alpha \left(\frac{\dot{\alpha}}{U_\infty} \right)^3 \right. \\ & + \alpha^3 + 3S' \left(\frac{\dot{h}}{U_\infty} \right)^2 \frac{\dot{\alpha}}{U_\infty} + 3 \left(\frac{\dot{h}}{U_\infty} \right)^2 \alpha + 3I'_\alpha \left(\frac{\dot{\alpha}}{U_\infty} \right)^2 \frac{\dot{h}}{U_\infty} + 3I'_\alpha \left(\frac{\dot{\alpha}}{U_\infty} \right)^2 \alpha \\ & \left. + 3\alpha^2 \frac{\dot{h}}{U_\infty} + 3S'\alpha^2 \frac{\dot{\alpha}}{U_\infty} + 6S' \frac{\dot{h}}{U_\infty} \frac{\dot{\alpha}}{U_\infty} \alpha \right) \quad (11) \end{aligned}$$

where

$$J'_\alpha = \frac{1}{4c} \left((c - x_f)^4 - x_f^4 \right) \quad (12)$$

$$\begin{aligned} m_{x_f}(t) = & -\frac{4\lambda q_\infty c}{M_\infty} \left(S' \frac{\dot{h}}{U_\infty} + I'_\alpha \frac{\dot{\alpha}}{U_\infty} + S' \alpha \right) - \frac{(\gamma + 1)\lambda^3 M_\infty q_\infty c}{3} \left(S' \left(\frac{\dot{h}}{U_\infty} \right)^3 \right. \\ & + K'_\alpha \left(\frac{\dot{\alpha}}{U_\infty} \right)^3 + S' \alpha^3 + 3I'_\alpha \left(\frac{\dot{h}}{U_\infty} \right)^2 \frac{\dot{\alpha}}{U_\infty} + 3S' \left(\frac{\dot{h}}{U_\infty} \right)^2 \alpha \\ & + 3J'_\alpha \left(\frac{\dot{\alpha}}{U_\infty} \right)^2 \frac{\dot{h}}{U_\infty} + 3J'_\alpha \left(\frac{\dot{\alpha}}{U_\infty} \right)^2 \alpha + 3S' \alpha^2 \frac{\dot{h}}{U_\infty} + 3I'_\alpha \alpha^2 \frac{\dot{\alpha}}{U_\infty} \\ & \left. + 6I'_\alpha \frac{\dot{h}}{U_\infty} \frac{\dot{\alpha}}{U_\infty} \alpha \right) \end{aligned} \quad (13)$$

where

$$S' = c/2 - x_f \quad (14)$$

$$I'_\alpha = \frac{1}{3} (c^2 - 3cx_f + 3x_f^3) \quad (15)$$

$$K'_\alpha = \frac{1}{5c} \left((c - x_f)^5 - x_f^5 \right) \quad (16)$$

4 HIGH SPEED NONLINEAR AEROELASTIC MODEL

The complete nonlinear aeroelastic smart wing system can be obtained by substituting Eqs. (11) and (13) into the equations of motion, Eq. (1) as follows

$$\begin{aligned} \mathbf{A}\ddot{\mathbf{y}} + \left(\mathbf{C} + \frac{2\lambda\rho_\infty U_\infty c}{M_\infty} \mathbf{D} \right) \dot{\mathbf{y}} + \left(\mathbf{E} + \frac{2\lambda\rho_\infty U_\infty^2 c}{M_\infty} \mathbf{F} \right) \mathbf{y} \\ + \frac{(\gamma + 1)\lambda^3 M_\infty q_\infty c}{3} \mathbf{G}\mathbf{g}(\dot{h}, \dot{\alpha}, \alpha) = \mathbf{0} \end{aligned} \quad (17)$$

where \mathbf{A} is the structural mass matrix, \mathbf{C} is the structural damping matrix, \mathbf{D} is the aerodynamic damping matrix, \mathbf{E} is the structural stiffness matrix, \mathbf{F} the aerodynamic stiffness matrix. Those matrices are defined as

$$\mathbf{A} = \begin{pmatrix} m & S_{\alpha h} & 0 & 0 \\ S_{\alpha h} & I_\alpha & 0 & 0 \\ 0 & 0 & L_h & 0 \\ 0 & 0 & 0 & L_\alpha \end{pmatrix} \quad (18)$$

$$\mathbf{C} = \begin{pmatrix} c_h & 0 & 0 & 0 \\ 0 & c_\alpha & 0 & 0 \\ 0 & 0 & R_h & 0 \\ 0 & 0 & 0 & R_\alpha \end{pmatrix} \quad (19)$$

$$\mathbf{D} = \begin{pmatrix} 1 & S' & 0 & 0 \\ S' & I'_\alpha & 0 & 0 \\ 0 & 0 & 0 & 0 \\ 0 & 0 & 0 & 0 \end{pmatrix} \quad (20)$$

$$\mathbf{E} = \begin{pmatrix} k_h & 0 & -\beta_h & 0 \\ 0 & k_\alpha & 0 & -\beta_\alpha \\ -\beta_h & 0 & \frac{1}{C_{p_h}} & 0 \\ 0 & -\beta_\alpha(x_f - x_p) & 0 & \frac{1}{C_{p_\alpha}} \end{pmatrix} \quad (21)$$

$$\mathbf{F} = \begin{pmatrix} 0 & 1 & 0 & 0 \\ 0 & S' & 0 & 0 \\ 0 & 0 & 0 & 0 \\ 0 & 0 & 0 & 0 \end{pmatrix} \quad (22)$$

$$\mathbf{G} = \begin{pmatrix} 1 & J'_\alpha & 1 & 3S' & 3 & 3I'_\alpha & 3I'_\alpha & 3 & 3S' & 6S' \\ S' & K'_\alpha & S' & 3I'_\alpha & 3S' & 3J'_\alpha & 3J'_\alpha & 3S' & 3I'_\alpha & 6I'_\alpha \end{pmatrix} \quad (23)$$

$$\mathbf{g}(\dot{h}, \dot{\alpha}, \alpha) = \left(\frac{\dot{h}^3}{U_\infty^3} \quad \frac{\dot{\alpha}^3}{U_\infty^3} \quad \alpha^3 \quad \frac{\dot{h}^2 \dot{\alpha}}{U_\infty^3} \quad \frac{\dot{h}^2 \alpha}{U_\infty^2} \quad \frac{\dot{\alpha}^2 \dot{h}}{U_\infty^3} \quad \frac{\dot{\alpha}^2 \alpha}{U_\infty^2} \quad \frac{\alpha^2 \dot{h}}{U_\infty} \quad \frac{\alpha^2 \dot{\alpha}}{U_\infty} \quad \frac{\dot{h} \dot{\alpha} \alpha}{U_\infty^2} \right)^T \quad (24)$$

There are many nonlinear terms in these equations with weak nonlinearity. The order of the linear and nonlinear aerodynamic coefficient terms are the same magnitude and \dot{h}/U_∞ , $\dot{\alpha}/U_\infty$ and α are small. Moreover, if $x_f < c/2$, all of the \mathbf{G} matrix elements are positive therefore, plunge hardening stiffness and plunge and pitch hardening damping can be created by the aerodynamic nonlinearity.

To calculate static divergence, one needs to consider $\ddot{\mathbf{y}} = \dot{\mathbf{y}} = \mathbf{0}$ in Eqs. (17) then

$$\left(\mathbf{E} + \frac{2\lambda\rho_\infty U_\infty^2 c}{M_\infty} \mathbf{F} \right) \mathbf{y} + \frac{(\gamma + 1)\lambda^3 M_\infty q_\infty c}{3} \begin{pmatrix} 1 \\ S' \end{pmatrix} \alpha^3 = \mathbf{0} \quad (25)$$

which in expanded form become

$$\begin{cases} K_h h + \frac{2\lambda\rho_\infty U_\infty^2 c}{M_\infty} \alpha + \frac{(\gamma + 1)\lambda^3 M_\infty q_\infty c}{3} \alpha^3 - \beta_h q_h = 0 \\ K_\alpha \alpha + \frac{2\lambda\rho_\infty U_\infty^2 c}{M_\infty} S' \alpha + \frac{(\gamma + 1)\lambda^3 M_\infty q_\infty c}{3} S' \alpha^3 - \beta_\alpha q_\alpha = 0 \\ \frac{1}{C_{p_h}} q_h - \beta_h h = 0 \\ \frac{1}{C_{p_\alpha}} q_\alpha - \beta_\alpha (x_f - x_p) \alpha = 0 \end{cases} \quad (26)$$

Considering the second and fourth equations, one can derive the static divergence as

$$K_\alpha + S' \left(\frac{2\lambda\rho_\infty U_\infty^2 c}{M_\infty} + \frac{(\gamma + 1)\lambda^3 M_\infty q_\infty c}{3} \alpha^2 \right) - C_{p_\alpha} \beta_\alpha^2 (x_f - x_p) = 0 \quad (27)$$

which by solving the nonlinear Eq. (27), the divergence velocity can be found $U_\infty(\alpha) = U_D(\alpha)$, the static divergence velocity at different pitch displacements α . If $x_f - x_p < 0$, since the entire term in the first bracket is positive, the static divergence can only happen when $S' < 0$ or $x_f > c/2$. By considering the piston theory, the aerodynamic center lies on the half-chord then S' is the distance between the half-chord and the pitch axis. In other words, static divergence or pitchfork bifurcation cannot happen if the pitch axis lies forward of the half-chord.

To estimate the smart wing limit cycles, equivalent linearisation needs to be applied to Eqs. (17). Due to having multiple nonlinearity, it needs to modify the methodology. To do so, the complete nonlinear aeroelastic system limit cycles are approximated by the following sinusoidal responses

$$\begin{aligned} h &= H \sin \omega t \\ \dot{h} &= \omega H \cos \omega t \\ \alpha &= A \sin \omega t \\ \dot{\alpha} &= \omega A \cos \omega t \end{aligned} \tag{28}$$

where H and A are the plunge and pitch amplitudes, respectively, and ω is the limit cycle frequency. Now all the nonlinear terms in $\mathbf{g}(\dot{h}, \dot{\alpha}, \alpha, U_\infty)$ needs to be written as a first order Fourier series

$$\mathbf{g}(\dot{h}, \dot{\alpha}, \alpha) = \mathbf{a}_0 + \mathbf{a}_1 \cos \omega t + \mathbf{b}_1 \sin \omega t \tag{29}$$

The Fourier coefficients can be presented as

$$\begin{aligned} a_{0_i} &= \frac{\omega}{2\pi} \int_{-\pi/\omega}^{\pi/\omega} \mathbf{g}_i(\omega H \cos \omega t, \omega A \cos \omega t, A \sin \omega t) dt \\ a_{1_i} &= \frac{\omega}{2\pi} \int_{-\pi/\omega}^{\pi/\omega} \mathbf{g}_i(\omega H \cos \omega t, \omega A \cos \omega t, A \sin \omega t) \cos \omega t dt \\ b_{1_i} &= \frac{\omega}{2\pi} \int_{-\pi/\omega}^{\pi/\omega} \mathbf{g}_i(\omega H \cos \omega t, \omega A \cos \omega t, A \sin \omega t) \sin \omega t dt \end{aligned} \tag{30}$$

where the notation a_{1_i} , \mathbf{g}_i and so on, represents the vector \mathbf{a}_1 , \mathbf{g} and so on i th element, for $i = 1, \dots, 10$. Since all the terms are polynomial, they are easy to integrate which leads to $\mathbf{a}_0 = 0$,

$$\mathbf{a}_1 = \begin{pmatrix} \frac{3H^3\omega^3}{4U_\infty^3} \\ \frac{3A^3\omega^3}{4U_\infty^3} \\ 0 \\ \frac{3AH^2\omega^3}{4U_\infty^3} \\ 0 \\ \frac{3A^2H\omega^3}{4U_\infty^3} \\ 0 \\ \frac{A^2H\omega}{4U_\infty} \\ \frac{A^3\omega}{4U_\infty} \\ 0 \end{pmatrix}, \quad \mathbf{b}_1 = \begin{pmatrix} 0 \\ 0 \\ \frac{3A^3}{4} \\ 0 \\ \frac{AH^2\omega^2}{4U_\infty^2} \\ 0 \\ \frac{A^3\omega^2}{4U_\infty^2} \\ 0 \\ 0 \\ \frac{A^2H\omega^2}{4U_\infty^2} \end{pmatrix} \quad (31)$$

In the nonlinear terms, six terms contribute to nonlinear damping since only involving the \mathbf{a}_1 coefficient, while the other four terms contribute to nonlinear stiffness. The complete nonlinear term $\mathbf{Gg}(\dot{h}, \dot{\alpha}, \alpha)$ in Eqs. (17) can be given as follows

$$\mathbf{Gg}(\dot{h}, \dot{\alpha}, \alpha) = \mathbf{G}(\mathbf{a}_0 + \mathbf{a}_1 \cos \omega t + \mathbf{b}_1 \sin \omega t) \quad (32)$$

For instance, the resulting vector first element which is the lift equation nonlinear term will be

$$\begin{aligned} & \frac{3H^3\omega^3}{4U_\infty^3} \cos \omega t + J'_\alpha \frac{3A^3\omega^3}{4U_\infty^3} \cos \omega t + \frac{3A^3}{4} \sin \omega t + 3S' \frac{3AH^2\omega^3}{4U_\infty^3} \cos \omega t \\ & + 3 \frac{AH^2\omega^2}{4U_\infty^2} \sin \omega t + 3I'_\alpha \frac{3A^2H\omega^3}{4U_\infty^3} \cos \omega t + 3I'_\alpha \frac{A^3\omega^2}{4U_\infty^2} \sin \omega t + 3 \frac{A^2H\omega}{4U_\infty} \cos \omega t \\ & + 3S' \frac{A^3\omega}{4U_\infty} \cos \omega t + 6S' \frac{A^2H\omega^2}{4U_\infty^2} \sin \omega t \end{aligned} \quad (33)$$

Stiffness and damping terms include the sine and cosine terms, respectively. Moreover, grouping them also leads to plunge stiffness and damping and pitch stiffness and damping terms. To do so, if the H order in a term is higher than that of A , one can consider it as a plunge term. The lift equation nonlinear term can be presented as follows

$$\begin{aligned} & \left(\frac{3H^2\omega^2}{4U_\infty^3} + 3S' \frac{3AH\omega^2}{4U_\infty^3} \right) \omega H \cos \omega t \\ & + \left(J'_\alpha \frac{3A^2\omega^2}{4U_\infty^3} + 3I'_\alpha \frac{3AH\omega^2}{4U_\infty^3} + 3 \frac{AH}{4U_\infty} + 3S' \frac{A^2}{4U_\infty} \right) \omega A \cos \omega t \\ & + 3 \frac{AH\omega^2}{4U_\infty^2} H \sin \omega t + \left(\frac{3A^2}{4} + 3I'_\alpha \frac{A^2\omega^2}{4U_\infty^2} + 6S' \frac{AH\omega^2}{4U_\infty^2} \right) A \sin \omega t \end{aligned} \quad (34)$$

The same way can be implemented to the moment equation nonlinear term. Then the complete nonlinear term can be represented as the sum of equivalent linear damping and stiffness by substituting from Eqs. (28)

$$\mathbf{Gg}(\dot{h}, \dot{\alpha}, \alpha) = \mathbf{C}_{eq}\dot{\mathbf{y}} + \mathbf{K}_{eq}\mathbf{y} \quad (35)$$

where

$$\mathbf{C}_{eq} = \frac{3}{4} \begin{pmatrix} \frac{H^2\omega^2}{U_\infty^3} + \frac{3S'AH\omega^2}{U_\infty^3} & \frac{J'_\alpha A^2\omega^2}{U_\infty^3} + \frac{3I'_\alpha AH\omega^2}{U_\infty^3} + \frac{AH}{U_\infty} + \frac{S'A^2}{U_\infty} \\ \frac{S'H^2\omega^2}{U_\infty^3} + \frac{3I'_\alpha AH\omega^2}{U_\infty^3} & \frac{K'_\alpha A^2\omega^2}{U_\infty^3} + \frac{3J'_\alpha AH\omega^2}{U_\infty^3} + \frac{S'AH}{U_\infty} + \frac{I'_\alpha A^2}{U_\infty} \end{pmatrix} \quad (36)$$

$$\mathbf{K}_{eq} = \frac{3}{4} \begin{pmatrix} \frac{AH\omega^2}{U_\infty^2} & A^2 + \frac{I'_\alpha A^2\omega^2}{U_\infty^2} + \frac{2S'AH\omega^2}{U_\infty^2} \\ \frac{S'AH\omega^2}{U_\infty^2} & S'A^2 + \frac{J'_\alpha A^2\omega^2}{U_\infty^2} + \frac{2I'_\alpha AH\omega^2}{U_\infty^2} \end{pmatrix} \quad (37)$$

and \mathbf{C}_{eq} and \mathbf{K}_{eq} are the matrices of the equivalent linear damping and stiffness, respectively. To obtain the complete equivalent linear aeroelastic system, it needs to substitute Eq. (35) into Eqs. (17)

$$\begin{aligned} \mathbf{A}\ddot{\mathbf{y}} + \left(\mathbf{C} + \frac{2\lambda\rho_\infty U_\infty c}{M_\infty} \mathbf{D} + \frac{(\gamma+1)\lambda^3 M_\infty q_\infty c}{3} \mathbf{C}_{eq} \right) \dot{\mathbf{y}} \\ + \left(\mathbf{E} + \frac{2\lambda\rho_\infty U_\infty^2 c}{M_\infty} \mathbf{F} + \frac{(\gamma+1)\lambda^3 M_\infty q_\infty c}{3} \mathbf{K}_{eq} \right) \mathbf{y} = \mathbf{0} \end{aligned} \quad (38)$$

In the present work, there are several nonlinearity of stiffness and damping including both of the DOF of system. Totally there are four unknowns as the two amplitudes H and A , the flutter speed of the equivalent linear system U_F and the flutter frequency of the equivalent linear system ω_F . One of the ways to solve the problem is to use the amplitude-based iteration scheme explaining in the next section [18, 19].

5 AMPLITUDE-BASED ITERATION SCHEME

In the amplitude-based iteration scheme, one of the amplitudes, H or A , can be chose as the master amplitude; here A is selected as the master amplitude. All values of A from 0 to A_{max} are considered and for each value, it needs to guess a value of H and ω . To obtain the equivalent linear system flutter speed and frequency, the guessed values of H and ω are substituted into Eqs. (38). Also, the response amplitude of h at flutter, H_F , is calculated. Obviously, the flutter values H_F and ω_F are not equal to the guessed values H and ω . This iteration is continued until reaching $\mathbf{J}^T \mathbf{J} = 0$, where

$$\mathbf{J} = \begin{pmatrix} H - H_F \\ \omega - \omega_F \end{pmatrix} \quad (39)$$

The complete step of the procedure is represented as

1. Where $A_0 = 0$ and $A_{n_A} = A_{max}$, the maximum pitch amplitude of interest, choose pitch amplitude values A_i for $i = 0, \dots, n_A$.
2. The solution for $A_0 = 0$ is known as a limit cycle vibration with zero amplitude which occur at the Hopf point, i.e. the linear flutter speed.
3. Guess $H = H_{i-1}$, $\omega_i = \omega_{i-1}$ for the i th amplitude A_i .
4. Using the equivalent linearized system of Eqs. (38), calculate the flutter speed U_F , flutter frequency ω_F and plunge amplitude H_F .
5. From Eq. (39), calculate \mathbf{J} .
6. If $\mathbf{J}^T \mathbf{J} < \varepsilon$ and $\varepsilon \ll 1$, increment i and go back to step 3.
7. If $\mathbf{J}^T \mathbf{J} < \varepsilon$, set $H = H_F$, $\omega = \omega_F$ and continue from step 4.

6 NUMERICAL EXAMPLE

For the high-speed smart wing shown in Fig. 1, considering the following parameters and using equivalent linearisation, estimate the bifurcation behaviour.

$m = 13.5 \text{ Kg}$	$S_{\alpha h} = 0.3375 \text{ Kgm}$	$c_h = 0.25 \text{ Ns/m}$
$I_\alpha = 0.0787 \text{ Kgm}^2$	$L_h = 1 \text{ H}$	$e_h = 0.145 \text{ C/m}$
$R_h = 1 \Omega$	$C_{ph} = 268 \mu\text{F}$	$L_\alpha = 300 \text{ H}$
$e_\alpha = 55.2 \text{ C/m}$	$R_\alpha = 1 \Omega$	$C_{p\alpha} = 36.8 \mu\text{F}$
$\rho = 1.225 \text{ Kg/m}^3$	$S' = 0.025 \text{ m}$	$I'_\alpha = 0.0058 \text{ m}^2$
$J'_\alpha = 1.0156 \times 10^{-4} \text{ m}^3$	$K'_\alpha = 1.3187 \times 10^{-5} \text{ m}^4$	$b = 0.125 \text{ m}$
$x_f = 0.4c$	$x_p = 0.1c$	$c = 0.25 \text{ m}$

By setting $\omega_h = 80 \text{ Hz}$ and $\omega_\alpha = 30 \text{ Hz}$, therefore, $K_h = 3.41 \times 10^6 \text{ N/m}$ and $K_\alpha = 2.80 \times 10^3 \text{ N/m}$. It assumes the structural damping matrix as $\mathbf{C} = \mathbf{E}/1000$, the speed of sound is constant at $a_\infty = 341 \text{ m/s}$, and $M_\infty = U_\infty/a_\infty$. Because of locating the pitch axis in front of the half-chord at $x_f = 0.4c$, there is no static divergence in the system. In the next step, the flutter speed of the underlying linear system is calculated. To calculate the flutter speed, the Hof test function needs to be detected as [13, 20]

$$\tau_H(U) = \prod_{j=1}^{n_c/2} (\lambda_{c,j}(U) + \lambda_{c,j}(U)^*) \quad (40)$$

where $\lambda_{c,j}$ and $\lambda_{c,j}^*$ are the j th complex conjugate eigenvalues pair and n_c is the complex eigenvalues total number. Hence, the Hopf test function, τ_H , represents the product of the real parts of the complex eigenvalues. A Hopf bifurcation, subcritical or supercritical, can occur when one of bracket term in Eq. (40) is equal to zero. Moreover, the Hopf test function becomes negative when the fixed point is unstable and vice-versa. Figure 2 demonstrates the smart wing underlying linear system is stable at low speeds and becomes unstabilised at the first flutter point at 355.6 m/s. However, the regular wing underlying linear system is unstable at low speeds and becomes stabilised at the first flutter point at 370.2 m/s. The smart wing has a second flutter point

at 999.7 m/s, after which the system becomes stable. However, the regular wing possesses a second flutter point at 749.7 m/s, after which the system becomes unstable.

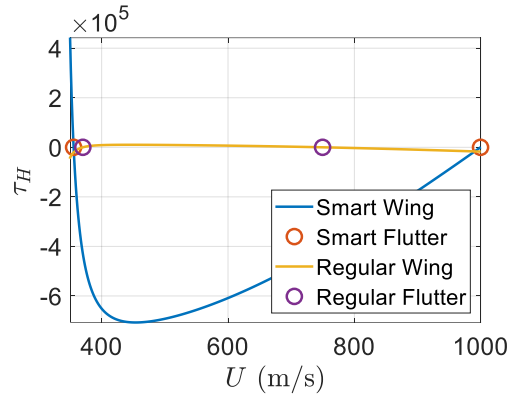
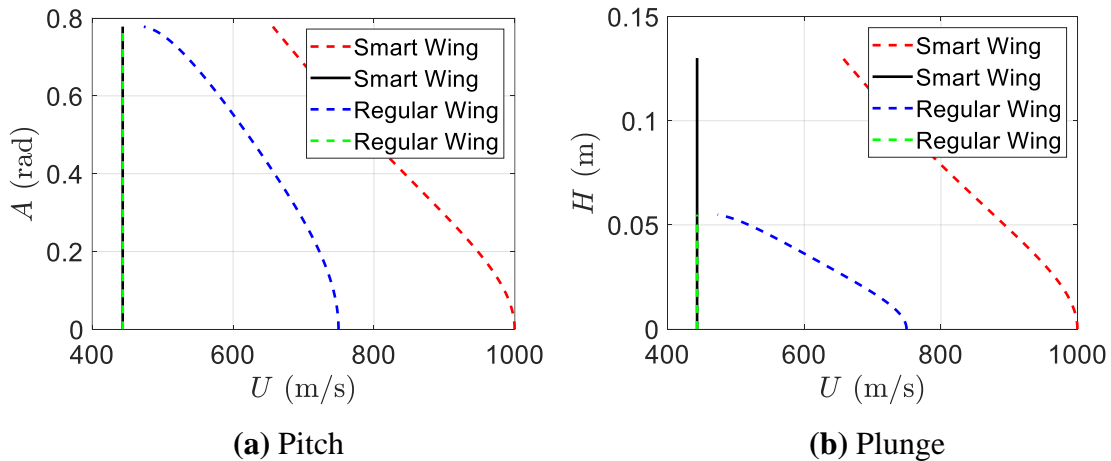
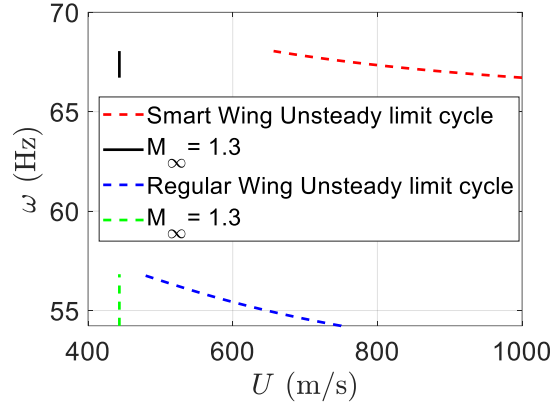


Fig. 2 Underlying linear system flutter test function

Since the first flutter points for both smart and regular wings are below the piston theory validity limit, $M_\infty = 1.3$, are not acceptable solutions. Hence, the second flutter points for both smart and regular wings become acceptable solutions. Implementing a piezoelectric patch on a wing can increase its flutter speed to $U_F = 999.7$ m/s, which shows 25% increase from the regular wing value and the corresponding frequency $\omega_F = 66.7$ Hz, indicating 23% increase from the regular wing value.

The amplitude-based iteration scheme is implemented at flutter point $U_F = 999.7$ m/s as explained previously. The pitch amplitude $A_{max} = 0.778$ rad is considered as the master amplitude and between 0 and A_{max} 200 nonlinear spaced values of A is selected and $\varepsilon = 10^{-8}$ is chosen as the convergence tolerance. The resulting limit cycle pitch and plunge amplitudes and frequency are depicted in Fig. 3.





(c) Frequency

Fig. 3 Pitch and plunge amplitude and frequency of limit cycle with nonlinear aerodynamics

The vertical lines show the piston theory validity limit, $M_\infty = 1.3$. To indicate the instability of the limit cycles, all curves are plotted in dashed lines. Both the amplitudes of the pitch and plunge are zero at the linear flutter speed, only to increase with decreasing speed. The maximum amplitude of pitch A_{max} for both the smart and regular wings occurs at 45° which is much higher than the usual maximum angle values investigated with piston theory; usually the validity of the pitch limit for piston theory is equal or less than 30° [14]. It is noticed that the smart wing maximum pitch amplitude is $A_{max} = 0.78$ rad happening at $U_{A_{max}} = 659.2$ m/s however, the regular wing maximum pitch amplitude is $A_{max} = 0.78$ rad occurring at $U_{A_{max}} = 473.4$ m/s, as shown in Fig. 3a. Furthermore, the rate of reduction of the pitch amplitude in the smart wing is lower than the one in the regular wing. Figure 3b depicts the smart wing maximum plunge amplitude is $H_{max} = 0.13$ m which happens at $U_{H_{max}} = 656.5$ m/s however, the regular wing maximum plunge amplitude is $H_{max} = 0.055$ m which occurs at $U_{H_{max}} = 473.4$ m/s, as depicted in Fig. 3b. The rate of reduction of the plunge amplitude in the smart wing is higher than the one in the regular wing.

The piston theory nonlinear terms do not cause instability in the smart wing by creating a subcritical Hopf bifurcation occurring at the linear flutter speed in the equivalent linearization. However, using the equivalent linearization can create instability in the regular wing at the linear flutter speed. Near the Hopf point, the resulting limit cycle oscillations are most dangerous because their amplitude is small then they can be easily increased.

As depicted in Fig. 3, the analysis of equivalent linearization is performed for pitch amplitudes up to $A_{max} = 0.778$. However, the amplitude-based algorithm cannot converge if $A_{max} = 0.8$. In other words, the smart wing pitch amplitude of limit cycle reaches a maximum value of 0.778 at 656.5 m/s but when airspeed decreases pitch amplitude decreases; similarly, the regular wing pitch amplitude of limit cycle reaches a maximum value of 0.778 at 473.4 m/s however, after decreasing airspeed pitch amplitude decrease.

To manage that problem, airspeed-based iteration scheme is considered as an alternative solution algorithm.

7 CONCLUSIONS

In this paper, it has been investigated aeroelastic phenomena of a smart wing in supersonic and hypersonic flows to represent the flutter alleviation due to piezoelectric effect. A smart wing with pitch and plunge DOFs is simulated by using nonlinear aerodynamic model. The equations of motion can be obtained by using the Lagrange's equations and the Kirchhoff's law. To calculate aerodynamic forces acting on the smart wing in supersonic flow, piston theory can be implemented to model airflow by a quasi-steady compressible method. The complete nonlinear aeroelastic smart wing system can be obtained and divergence and flutter speeds are calculated accordingly. The results indicate a considerable achievement in dynamic aeroelastic behavior of a wing.

REFERENCES

- [1] N. Nguyen, et al., "Aeroelastic Analysis of a Flexible Wing Wind Tunnel Model with Variable Camber Continuous Trailing Edge Flap Design", AIAA 2015-1405, 2015.
- [2] B. P. Hallissy, C. E. S. Cesnik, "High-fidelity Aeroelastic Analysis of Very Flexible Aircraft", AIAA 2011-1914, 2011.
- [3] R. L. Bisplinghoff, et al., "Aeroelasticity", Republication, Dover Publications, 1996.
- [4] Y. C. Fung, "An Introduction to the Theory of Aeroelasticity", Republication, Dover Publications, 2008.
- [5] E. H. Dowell, "A Modern Course in Aeroelasticity", 5th Ed., Springer International Publishing Switzerland, 2015.
- [6] D. H. Hodges, G. A. Pierce, "Introduction to Structural Dynamics and Aeroelasticity", 2nd Ed., Cambridge University Press, 2011.
- [7] J. R. Wright, J. E. Cooper, "Introduction to Aircraft Aeroelasticity and Loads", 2nd Ed., John Wiley & Sons, Ltd., 2015.
- [8] E. Verstraelen, et al., "Flutter and limit cycle oscillation suppression using linear and nonlinear tuned vibration absorbers", Proceedings of the SEM IMAC XXXV, 2017.
- [9] B. Lossouarn, et al., "Design of inductors with high inductance values for resonant piezoelectric damping", Sensors and Actuators A: Physical 259, 68-76, 2017.
- [10] R. Moosavi and E. Faris, "Smart Wing Flutter Suppression" Designs, 6(2), 29, 2022.
- [11] R. Moosavi, "Smart Blade Flutter Alleviation with Rotational Effect", Designs, 6(5), 98, 2022.
- [12] R. Moosavi, "Smart Blade Flutter Alleviation", Engineering with Computers, 39(6), 2023.
- [13] M. Lighthill, "Oscillating airfoils at high mach numbers", Journal of Aeronautical Science 20(6), 402-406, 1953.
- [14] D.D. Liu, Z.X. Yao, D. Sarhaddi, and F. Chavez, "From piston theory to a unified hypersonic-supersonic lifting surface method", Journal of Aircraft 34(3), 304-312, 1997.
- [15] V. Rao, A. Behal, P. Marzocca, and C. Rubillo, "Adaptive aeroelastic vibration suppression of a supersonic airfoil with flap", Aerospace Science and Technology 10(4), 309-315, 2006.

- [16] L.K. Abbas, Q. Chen, K. O'Donnell, D. Valentine, and P. Marzocca, "Numerical studies of a non-linear aeroelastic system with plunging and pitching freeplays in supersonic /hypersonic regimes", *Aerospace Science and Technology* 11(5), 405–418, 2007.
- [17] A. Gelb and W.E.V. Velde, "Multiple-Input Describing Functions and Nonlinear System Design", McGraw-Hill Book Company, New York, 1968.
- [18] R.M. Laurenson and R.M. Trn, "Flutter analysis of missile control surfaces containing structural nonlinearities", *AIAA Journal* 18(10), 1245–1251, 1980.
- [19] R. Seydel, "Practical Bifurcation and Stability Analysis", 3rd Ed. Springer, New York-Dordrecht-Heidelberg London, 1994.
- [20] S.G. Abel and N.K. Cooperrider, "An equivalent linearization algorithm for nonlinear system limit cycle analysis", *Journal of Dynamic Systems, Measurement, and Control* 107, 117–122, 1985.

COPYRIGHT STATEMENT

The author confirms that he, and/or his company or organisation, hold copyright on all of the original material included in this paper. The author also confirms that they have obtained permission from the copyright holder of any third-party material included in this paper to publish it as part of their paper. The author confirms that he give permission, or has obtained permission from the copyright holder of this paper, for the publication and public distribution of this paper as part of the IFASD 2024 proceedings or as individual off-prints from the proceedings.